Stabilization of minerals by reaction with phosphoric acid - Evolution of model compounds

Blandine Bournonville, Ange Nzihou, P Sharrock, G Depelsenaire

STABILIZATION OF MINERALS BY REACTION WITH PHOSPHORIC ACID
Evolution of Model Compounds

B. BOURNONVILLE[1†], A. NZIHOU[1*], P. SHARROCK[2] and G. DEPELSENAIRE[3]

[1]*LGPSD UMR CNRS 2392, Ecole des Mines d'Albi-Carmaux, Route de Teillet 81013 Albi CT Cedex 09, France*
[2]*LCBM, Université Paul Sabatier, Castres Cedex, France*
[3]*HSE (Health, Safety, Environment), Direction Centrale Recherche et Technologie, SOLVAY, Brussels, Belgium*

The mechanisms of heavy metal stabilization from mineral residues were investigated. The reaction of phosphoric acid with municipal waste incinerator fly ashes and some of its major constituents was assessed. The reaction was monitored by analysis of soluble phosphate contents as a function of time, as well as by pH and temperature variations. Evolution of the solids was followed by X-ray diffraction. Various phosphoric acid concentrations were used and yielded different end products for the case of lime and limestone. Silica and calcium sulphate were found to remain inert, while alumina consumed part of the soluble phosphate. Melilite showed a complex process of dissolution and precipitation of amorphous aluminium phosphates. These results help on understanding the phosphate reaction used to stabilize a mineral matrix like fly ash and demonstrate that insoluble minerals are formed such as calcium phosphates which may effectively trap heavy metal ions.

Keywords: kinetics; mineral matrix stabilization; fly ash; characterization; phosphate reaction.

INTRODUCTION

Municipal solid waste incineration (MSWI) generates fly ash residues which contain soluble chlorides and heavy metal pollutants (Derie, 1996; Eighmy *et al.*, 1997; Iretskaya *et al.*, 1999). Currently, much fly ash is landfilled following a cement solidification procedure (Andac and Glasser, 1998; Barth and Barich, 1995). An alternative treatment uses phosphoric acid to neutralize fly ash basicity and to form stable minerals including metal phosphates (Derie, 1996). This process is applied to flue gas filtration residus with no previous gas treatment and comprises the following steps: initially, the fly ash is washed and filtered to extract soluble salts (mostly chlorides). Then, phosphoric acid is added to the water-washed fly ash. After reaction, a thermal treatment dries the residues and transforms the solids into stable mineral species (Derie and Depaus, 1999). Such products may be safely landfilled or reused as mineral fillers. This report focuses on the phosphoric acid treatment which is central to the process and controls the final product's stability.

*Correspondence to: Dr A. Nzihou, LGPSD UMR CNRS 2392, Ecole des Mines d'Albi-Carmaux, Route de Teillet 81013 Albi CT cedex 09, France. E-mail: nzihou@enstimac.fr

†Present address: SDI/LPTh, CEA Le Ripault, BP 16, 37 260 Monts, France.

The aim of the phosphate addition is to form solid phosphates which can immobilize heavy metals (Haguenauer *et al.*, 1995; Admassu and Breese, 1999). Apatites were previously studied to immobilize heavy metal from water (Ma *et al.*, 1994a, b; Mavropoulos *et al.*, 2002; Leyva *et al.*, 2001; Fuller *et al.*, 2002), soil (Laperche *et al.*, 1996; Zhang *et al.*, 1997) or bottom ash (Crannell *et al.*, 2000). Calcium orthophosphates with high Ca/P ratios such as hydroxyapatite and tricalcium phosphate are typically insoluble in natural environments. Fly ashes are complex in composition (Le Forestier and Libourel, 1998). Water washed fly ash contains mainly silicoaluminates, calcium sulphates and carbonates, and also traces of heavy metals. The reaction sought during phosphate treatment of fly ash is the formation of insoluble di and trivalent metal phosphates. Such phosphates may form directly by reaction with mobilizable heavy metals, or may precipitate following a complex series of dissolution, neutralization and salt formation reactions.

We investigated the reaction of phosphoric acid with two different washed fly ashes. To better understand the reaction of water washed fly ash, we undertook the study of the reaction of phosphoric acid with different isolated fly ash components. The pure components chosen are Al_2O_3, SiO_2, $CaSO_4{-}2H_2O$, $CaCO_3$ and $Ca(OH)_2$. No chloride containing species were studied because the water extraction in the first step of the process was designed to remove

chlorides as much as possible. A more complex component, an amorphous calcium silicoaluminate, of melilite composition was also investigated. We now report on the individual binary reactions which illustrate the various behaviours encountered during fly ash treatment with phosphoric acid.

EXPERIMENTAL SECTION

The phosphoric acid used contained 85% acid and was a viscous liquid of density 1.7 g cc^{-1}. It was purchased as a Normapur product from Prolabo. The chemical compositions of the two washed fly ashes, named S and O, are presented in Table 1. These ashes originated from two different French MSWIs, and were collected as fly ash filtered prior to any gas treatment. They were water washed before phosphate reaction. These fly ashes were powders with a mean particle size of 24 μm and 44 μm for S and O fly ashes, respectively. Calcium salts were reagent grade and used as fine powders. Silica particles were of 50 μm diameter for chromatographic purposes. Melilite was a gift from the BRGM (French geological survey in Orleans) and contained 38% silica, 36% calcium oxide and 16% alumina as major components. It was used as a fine ball milled product. The particle sizes of each initial product are shown in Table 2.

A closed batch reactor was used to follow phosphoric acid reaction kinetics with selected compounds. It consisted in a 1 l Pyrex thermostatic vessel of 10 cm inner diameter equipped with a stainless steel double spire helicoidal mixer of 1 cm width and 5 cm outermost diameter. The rotational speed was controlled at 400 or 800 rpm. Data acquisition was monitored with a Mettler Toledo LABMAX® instrument. Experimental parameters included temperature, pH, time, mixing speed and mass of added phosphoric acid.

All reactions were carried out with 371.4 g of deionized water previously thermostated between 20–60°C during 5 min in the reaction vessel (Bournonville, 2002). 200 g of washed fly ash were put into water. 30 g of solids were used for alumina and calcium hydroxide. 50 g were used in the case of silica and melilite, 74 g for calcium sulphate and 90 g for calcium carbonate. These masses correspond to their approximate proportions in fly ash. Table 2 summarizes experimental data. The suspensions were homogenized during 5 min then 0, 16, 24 or 32 g of phosphoric acid were pumped in over a 1 min period. Thus, the initial phosphate concentrations were 0, 453, 680 or 907 mmol l^{-1}. To simplify graphics, the concentration of 453 mmol l^{-1} will be noted C′ and the other concentrations will be relative to C′. Samples were taken regularly and filtered immediately under vacuum at 0.45 μm. During the first 5 min, sampling intervals were 1 min, then 2 min. for the following 10 min, then 5 min up to 60 min. A final sample was taken at 80 min, and the filtered solids were dried in an oven at 105°C for 24 h.

Table 1. Chemical composition of fly ashes.

	Al_2O_3	CaO	Fe_2O_3	SiO_2	SO_4
S fly ash	9%	25%	8%	18%	20%
O fly ash	17%	25%	2%	28%	2%

Table 2. Experimental conditions.

	d50 (μm)	Mass added (g)	MMM (g mol^{-1})	Solid/liquid (%)	(Ca,Al,Si)/P
Al_2O_3	4.9	30	102	8.1	1.80 → 3.60
$CaCO_3$	24.4	90	100	24.2	2.76 → 5.51
$Ca(OH)_2$	5.0	30	74	8.1	1.24 → 2.48
$CaSO_4{-}2H_2O$	19.0	74	172	19.9	1.32 → 2.64
Melilite	44.4	50	274	13.5	≈0.20 → 0.40
SiO_2	41.0	50	60	13.5	2.55 → 5.10
S fly ash	23.6	200		53.8	
O fly ash	43.6	200		53.8	

X-ray diffraction (XRD) patterns of disoriented powders were registered with Ni filtered Cu Kα radiation (1.543 Å) on a Siemens D5000 diffractometer operating at 40 kV and 30 mA. The acquisition time for the patterns, in the 2θ 4–84° interval, was set at 3 s per step of 0.02°. The crystalline phases of the samples were indexed by comparison with standard JCPDS files. Soluble phosphate was determined by UV spectrophotometry by the molybdovanadate method with a detection limit of 0.02 mmol l^{-1} of PO_4. Sulphates were analysed by ion chromatography and other elements by atomic absorption.

RESULTS AND DISCUSSION

Fly Ashes

Water washed fly ashes remained basic: the pH of suspensions stabilized near pH 10 after their introduction in the reactor (Figure 1). When phosphoric acid was added to fly ash suspensions, carbon dioxide was released with the formation of foam (Derie and Depaus, 1999). With phosphoric acid addition, the pH dropped to 3.5 and then slowly rose to nearly neutral pH. Similar pH evolutions were obtained with the two different fly ashes studied.

The soluble phosphate consumption by fly ash is represented in Figure 2. Most phosphoric acid was consumed during the first minutes of the reaction. The reaction with S fly ash was slightly slower than that with O fly ash. More than half of the soluble phosphate was consumed during the first minute of reaction. The reaction speed decreased with time until all soluble phosphate disappeared. The reaction between the fly ashes and phosphoric

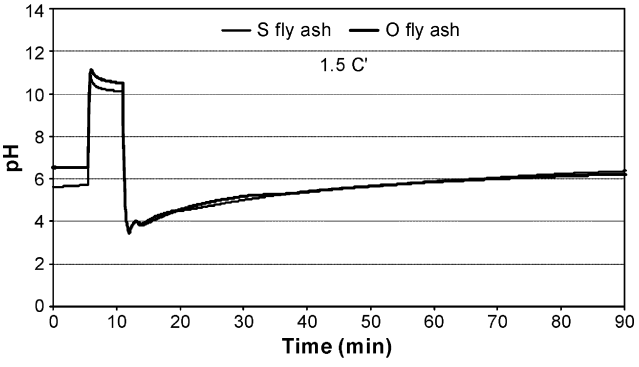

Figure 1. pH of the suspension during reaction between H_3PO_4 and fly ashes at 20°C, 400 rpm and phosphate concentration of 1.5 C′. C′: 453 mmol l^{-1} of phosphoric acid.

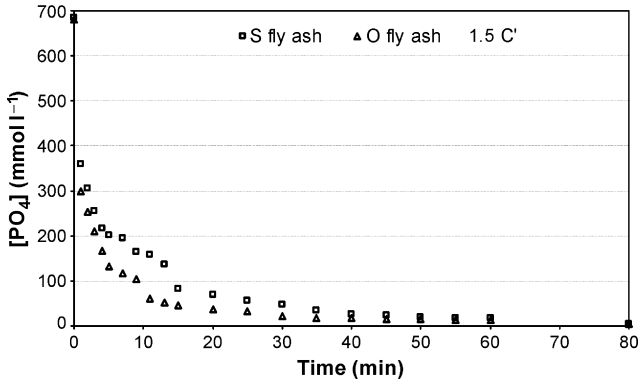

Figure 2. PO_4^{3-} in solution during reaction between H_3PO_4 and fly ashes at 20°C, 400 rpm and phosphate concentration of 1.5 C′. C′: 453 mmol l^{-1} of phosphoric acid.

acid was exothermal. When the acid was added, the temperature rose between 6–11°C for both fly ashes depending on the acid concentration. Further details, reaction kinetics and rheological studies were presented previously (Bournonville, 2002; Bournonville *et al.*, 2004).

This reaction between phosphoric acid and fly ashes is difficult to interpret because of the complex composition of the ashes. The study of the same reaction using model compounds under analogous conditions should help to understand the global phosphate reaction with fly ashes. Results pertaining to the reactivity of the six selected compounds are presented below in order of increasing complexity and starting with the least reactive ones.

Silica

As expected, silica is relatively inert towards phosphoric acid. There was a slight decrease in free phosphate concentration during the first minute of mixing, which amounts to approximately 6% of the acid introduced. Afterwards, soluble phosphate concentration was constant (Figure 3). The observed pH immediately decreased from neutral to 1 and stayed constant afterwards. The maximum concentration of Si was found to be 1.2 mmol l^{-1}. The temperature increase upon phosphoric acid addition was 1.5°C, which corresponds to the heat of dilution of the acid in the available water. There was no observable chemical reaction between silica and phosphoric acid in aqueous medium. The decrease in phosphate concentration may be attributed to the adsorption of phosphate molecules on or inside the porous silica structures. The only noticeable change was the decrease by one half in soluble silica in the presence of phosphoric acid (from 1.2 mmol l^{-1} to 0.6 mmol l^{-1}).

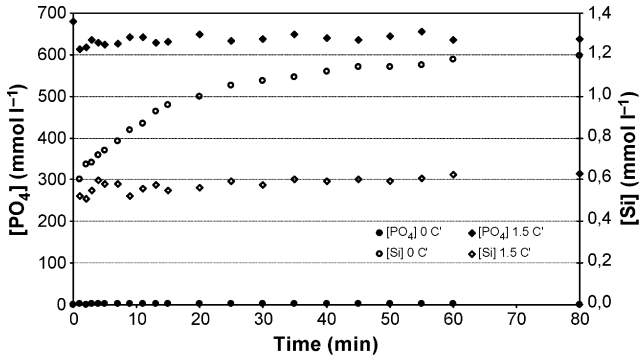

Figure 3. PO_4^{3-} and SiO_4^{4-} in solution during reaction between H_3PO_4 and SiO_2 at 20°C and 400 rpm. C′: 453 mmol l^{-1} of phosphoric acid.

Calcium Sulphate Hydrate

Calcium sulphate is sparingly soluble in water. We found an aqueous concentration of 16 mmol l^{-1} under our experimental conditions. This value corresponds to a solubility product constant pKs of 3.6 compared to literature equilibrium value of pKs of 4.5. No reaction was observed when phosphoric acid was added. Experimentally, the concentration of acid was unchanged at 98 ± 5% of the initial value (Figure 4). The pH levelled at pH 1 and did not change with temperature or speed of mixing. The acid conditions caused dissolution of some calcium sulphate. With 680 mmol l^{-1} of phosphoric acid, calcium and sulphate were found at 35 mmol l^{-1} concentrations at room temperature (20°C) and 50 mmol l^{-1} at 60°C. This dissolution represents less than 5% of the calcium sulphate introduced in the reaction vessel. These results are logical; indeed, phosphoric acid is manufactured by addition of sulphuric acid to phosphate rock (Gilbert and Moreno, 1965; Gioia *et al.*, 1977). At the observed concentrations and pH, a small amount of soluble calcium dihydrogenphosphate is formed. X-ray analysis of the filtered solids showed the remaining calcium sulphate was not contaminated with crystalline phosphates. The following equilibrium is present:

$$\begin{aligned} CaSO_4 - 2H_2O(s) + 2H_3PO_4(aq) \\ \rightarrow Ca(H_2PO_4)_2(aq) + H_2SO_4(aq) \\ + 2H_2O(aq) \end{aligned} \quad (1)$$

When phosphoric acid is added, the concentrations of calcium and sulfate are higher than those expected from the solubility products. At highly acidic pH values, crystallization of calcium phosphates is prevented, as previously discussed for similar systems (Zhang and Ryan, 1998).

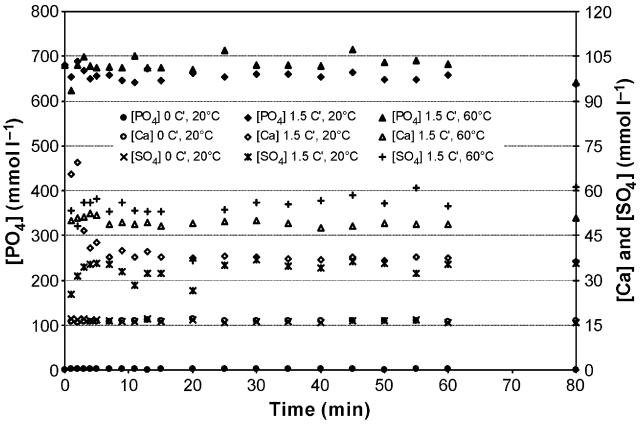

Figure 4. PO_4^{3-}, Ca^{2+} and SO_4^{2-} in solution during reaction between H_3PO_4 and $CaSO_4{-}2H_2O$ at 20°C or 60°C and 400 rpm. C′: 453 mmol l^{-1} of phosphoric acid.

Alumina

During the reaction of phosphoric acid with Al_2O_3, between 50–80 mmol l^{-1} of phosphate were consumed during the first 3 min as shown in Figure 5 which illustrates soluble phosphate concentrations as a function of time for various reaction conditions. This represents between 7–12% of the phosphoric acid added to the suspension. After 3 min, the free phosphate concentration in solution was nearly constant: the observed variation was less than 5% of the mean value and close to the measurement error. Modification of the stirring speed did not change the consumed phosphate quantity.

The initial pH of the suspension of Al_2O_3 in water was close to 10. This pH slowly decreased with time by neutralization of the solution with atmospheric CO_2. On the other hand, when phosphoric acid was added, the pH immediately dropped to pH 1 and remained constant. As illustrated in Figure 5, there was a slow dissolution of alumina with time and with the acidity of the suspension. This dissolution rate did not change with the variation of the stirring speed. No more than 15% by weight of Al_2O_3 dissolved after 80 min under acid conditions. The aluminium concentration ranged between 70–120 mmol l^{-1}. At the beginning of the experiment, under alkaline conditions, the aluminum concentration was constant near 0.1 mmol l^{-1}, well above our detection limit of 0.01 mmol l^{-1}.

The temperature of the suspension increased slightly with the addition of phosphoric acid. The larger was the quantity of acid, the more the temperature increased: 1.6°C for 453 mmol l^{-1}, and 3°C for 907 mmol l^{-1} of added phosphoric acid. This temperature rise is attributed to the exothermal dilution of acid in water.

The XRD pattern of the alumina used showed that initially, there was an appreciable content of Bayerite, $Al(OH)_3$. The quantity of this hydroxide decreased with phosphate addition while the oxide crystallinity remained constant. No crystalline aluminium phosphates were detected by XRD. The constant quantity of phosphate consumed seems to be related to the amount of Bayerite present. Reaction with phosphoric acid may occur on the surfaces of the particles with the formation of an insoluble and amorphous combination of phosphate and aluminium. Due to the presence of excess acid some aluminium dissolves by the formation of an acid aluminium hydrogenophosphate, $Al(H_2PO_4)_3$, according to the reaction of equation (2).

$$Al(OH)_3(s) + 3H_3PO_4(aq) \rightarrow Al(H_2PO_4)_3(aq) + 3H_2O(aq) \quad (2)$$

This dissolution is hindered by the insolubility of other aluminium orthophosphates which most probably coat the remaining alumina particles. The formation of $AlPO_4$ was reported previously (Crannell *et al.*, 2000), and is expected to occur as a surface complex on the basic aluminium hydroxide particles. However, at pH 1 in the solution phase, only dihydrogenophosphates may form.

Calcium Hydroxide

Up to 907 mmol l^{-1} phosphoric acid was rapidly consumed by calcium hydroxide suspensions in water. As illustrated in Figure 6, 90% of the phosphate was consumed during the first 5 min of reaction, the remainder being consumed later. A complex series of acid–base neutralization reactions occur, depending on the acid/base ratio. The variations in calcium and phosphate ion concentrations as a function of added phosphoric acid are presented in Figure 6. Calcium hydroxide alone stabilised near pH 13 under our experimental conditions with soluble calcium contents of 21 mmol l^{-1} (see in Figure 6, curve [Ca] 0 C′). This corresponds to an apparent pKs of 3.4, significantly different from the equilibrium pKs value of 5.3 for very pure powder. With 453 mmol l^{-1} phosphoric acid, the calcium ion concentration fluctuated but finally stabilized near 25 mmol l^{-1}. With higher acid concentrations, calcium dissolved initially, then precipitated out of solution, the final calcium concentrations being well below 10 mmol l^{-1}. Most of the calcium and phosphate ions were consumed during the first 10 min of reaction at room temperature, and then equilibrium was reached progressively during the next hour of mixing. The pH changes occurring while the reaction proceeds are shown in Figure 7. It can be seen that phosphoric acid caused a pH drop which is due to the neutralization of the soluble base. Next, the pH gradually increased and became stable after 1 h of stirring. With 907 mmol l^{-1} phosphoric acid, the pH stabilized near pH 5.5. When there was less phosphoric acid added, the final pH was higher: 8.5 or 13 with 680 or 453 mmol l^{-1} phosphoric acid, respectively.

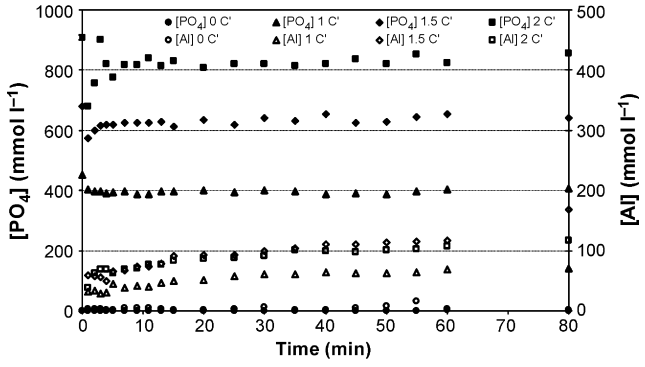

Figure 5. PO_4^{3-} and Al^{3+} in solution during reaction between H_3PO_4 and Al_2O_3 at 20°C and 400 rpm. C′: 453 mmol l^{-1} of phosphoric acid.

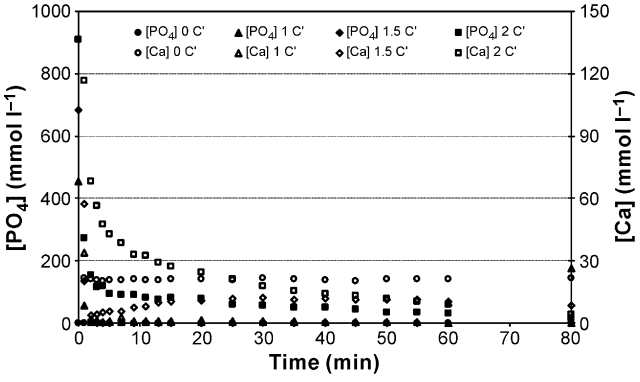

Figure 6. PO_4^{3-} and Ca^{2+} in solution during reaction between H_3PO_4 and $Ca(OH)_2$ at 20°C and 400 rpm. C′: 453 mmol l^{-1} of phosphoric acid.

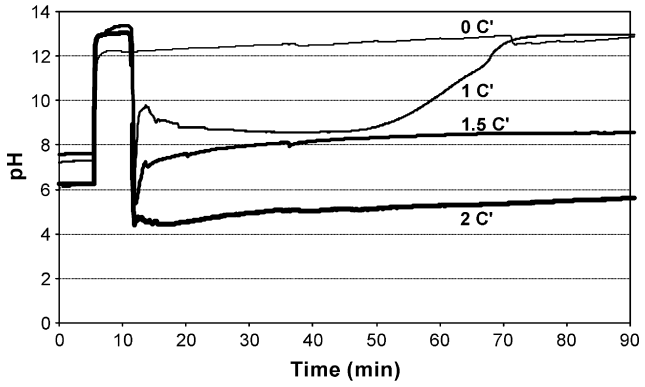

Figure 7. pH of the suspension during reaction between H_3PO_4 and $Ca(OH)_2$ at 20°C and 400 rpm. C′: 453 mmol l^{-1} of phosphoric acid.

These reactions were also followed by measuring the temperature evolutions. With 453 mmol l^{-1} phosphoric acid, the temperature rose by 5.8°C, while for 907 mmol l^{-1} phosphoric acid, it rose 17.1°C. Clearly, the acid–base reaction is exothermal and the temperature change related to the variation in pH. Four phenomena contribute to the temperature rise: phosphoric acid dilution, calcium hydroxide dissolution, acid–base neutralization and precipitation of calcium phosphates. Similar evolutions were reported recently in a study of the precipitation of hydroxyapatite particles from aqueous solutions (Bernard *et al.*, 1999, 2000).

XRD analysis of the end products in the solid phase helps identify the nature of the reaction. As illustrated in Figure 8, the starting lime product was well crystallized but contained traces of carbonate. Following reaction with 453 mmol l^{-1} of phosphoric acid, all the starting material was transformed into a mostly amorphous product of apatite like structure. With 680 mmol l^{-1} acid, both brushite ($CaHPO_4-2H_2O$) and octocalcium phosphate ($Ca_8H_2(PO_4)_6-5H_2O$) were formed. With excess acid, only brushite was found in the solid phase. The formation of calcium phosphates is known to depend on the stoichiometry of the reactants and on the pH of the solution in contact with the solids (Hudson and Dolan, 1982; Van Kemenade and de Bruyn, 1987). The equilibria are represented by equations (3)–(6).

$$Ca(OH)_2(s) + 2H_3PO_4(aq) \rightarrow Ca(H_2PO_4)_2(aq) + 2H_2O(aq) \quad (3)$$

$$Ca(H_2PO_4)_2(aq) + 2H_2O(aq) \longleftrightarrow CaHPO_4 - 2H_2O(s) + H_3PO_4(aq) \quad (4)$$

$$8CaHPO_4 - 2H_2O(s) \rightarrow Ca_8H_2(PO_4)_6 - 5H_20(s) + 2H_3PO_4(aq) + 11H_2O(aq) \quad (5)$$

$$5Ca_8H_2(PO_4)_6 - 5H_2O(s) \rightarrow 4Ca_{10}(PO_4)_6(OH)_2(s) + 6H_3PO_4(aq) + 17H_2O(aq) \quad (6)$$

Hydroxyapatite ($Ca_{10}(PO_4)_6(OH)_2$) is thermodynamically the most stable calcium phosphate at neutral or basic pH (Piantone *et al.*, 2003). Other calcium phosphates, including hydrogenophosphates, will revert to apatite by incongruent dissolution in sufficient water to evacuate excess phosphate. In a closed batch reactor such as in our case, the nature of the end products is determined by the final pH and the relatively moderate solubility of brushite. In any case, the calcium hydroxide reacts completely with proper mixing of the suspensions.

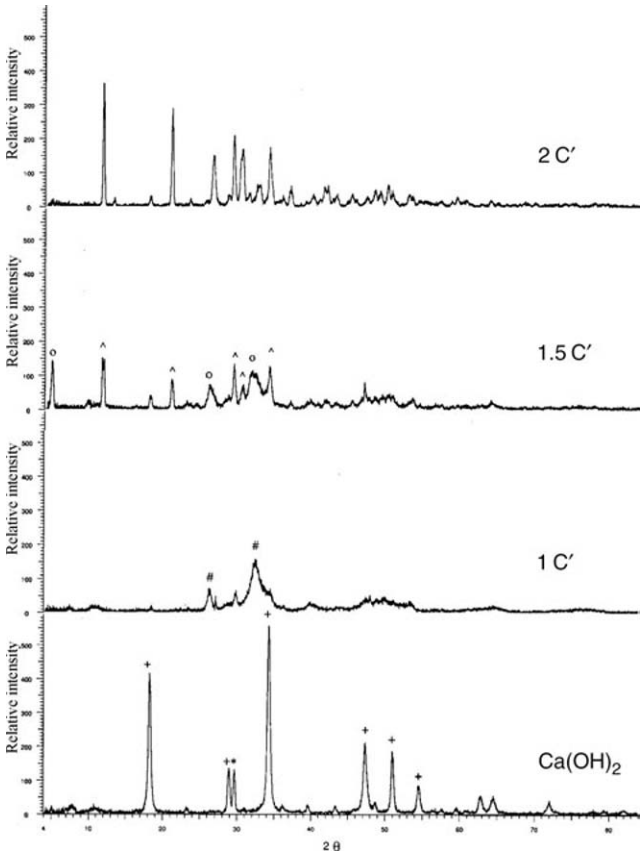

Figure 8. X-ray diffraction patterns of $Ca(OH)_2$ after phosphate reaction at variable rate. C′: 453 mmol l^{-1} of phosphoric acid. +: Lime ($Ca(OH)_2$); *: calcite ($CaCO_3$); ^: brushite ($CaHPO_4-2H_2O$); #: amorphous calcium apatite phosphate; ○: octocalcium phosphate ($Ca_8H_2(PO_4)_6-5H_2O$).

Calcium Carbonate

Less than 3 min were needed to consume all the phosphoric acid added to the calcium carbonate suspension at 20°C (Figure 9). Gaseous CO_2 was evolved and the reactions were moderately exothermal (2.3–4°C temperature rise). At 60°C, only 1 min was required to consume the acid. Less than 1.6 mmol l^{-1} of phosphate remained at the end of the experiments (our detection limit was 0.1 mmol l^{-1}). Addition of phosphoric acid caused the pH to drop below pH 4 in all cases, but only for 1 or 2 min (Bournonville *et al.*, 2001). The pH then rose to a plateau at pH 6. This is attributed to the buffering action of saturated aqueous carbonate anions. The kinetics of free phosphate concentrations as a function of temperature yielded a small activation energy of 15.8 kJ mol^{-1}, corresponding to an acid–base neutralization reaction. Pure calcium carbonate is insoluble in water. We found 0.4 mmol l^{-1} calcium concentrations

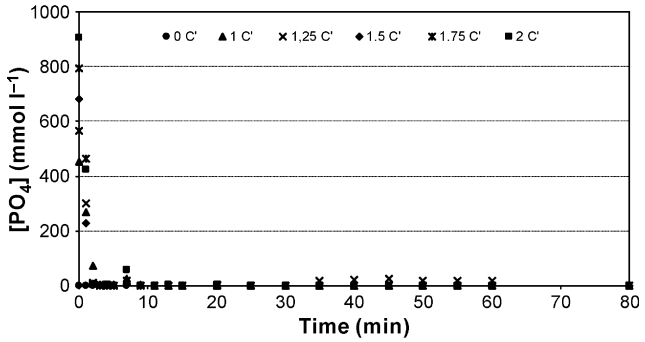

Figure 9. PO_4^{3-} in solution during reaction between H_3PO_4 and $CaCO_3$ at 20°C and 400 rpm. C′: 453 mmol l^{-1} of phosphoric acid.

(with a 0.05 mmol l^{-1} detection limit) which leads to an observed pKs of 6.8 compared to the literature's pKs of 8.3. During the first few minutes of reaction, while the pH was low, calcium concentrations reached 200 mmol l^{-1} levels before falling back to 7 mmol l^{-1}. Heating caused a further decrease to 3.5 mmol l^{-1}. Increasing the stiring speed slightly accelerated the phosphate reaction. XRD analysis of the end products revealed calcium carbonate was still present, even with 907 mmol l^{-1} phosphoric acid and heating (see Figure 10). The main calcium carbonate peak decreased in intensity by 50%, and small peaks due to octocalcium phosphate were detected. Most reaction products seemed to be amorphous, as confirmed by the presence of the broad apatite like peaks near 2θ values of 32°. The solution equilibrates with a complex mixture of mostly non-crystalline solids.

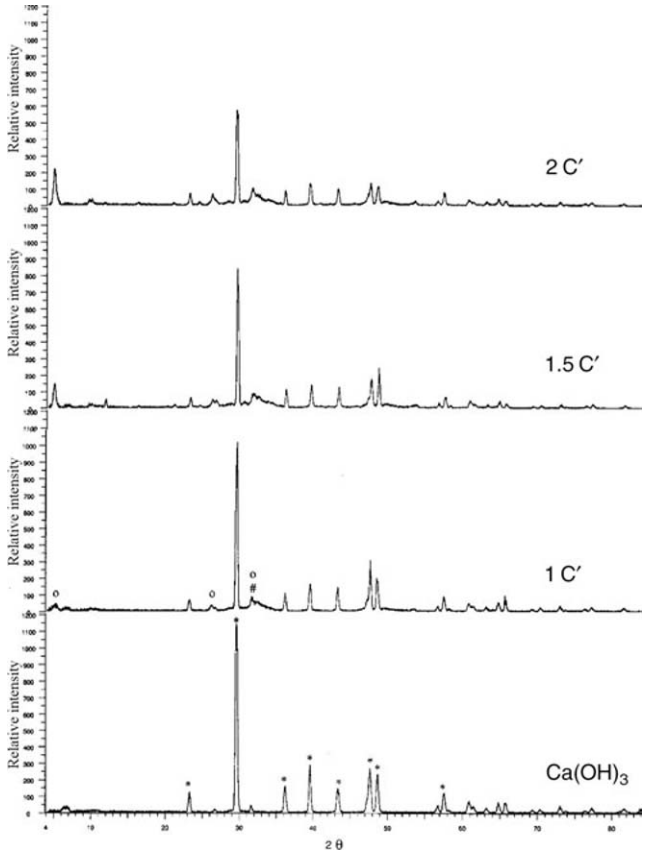

Figure 10. X-ray diffraction patterns of $CaCO_3$ after phosphate reaction at variable rate. C′: 453 mmol l^{-1} of phosphoric acid. *: Calcite ($CaCO_3$); #: amorphous calcium apatite phosphate, ○: octocalcium phosphate ($Ca_8H_2(PO_4)_6{-}5H_2O$).

The results are interpreted in terms of a dissolution–precipitation mechanism controlled by pH and stirring speed. We can account for the remaining carbonate solid by proposing it is trapped inside a shell of insoluble phosphate. Calcium carbonate is known to react slowly with calcium phosphates (Piantone *et al.*, 2003) according to the following equations.

$$6CaHPO_4 - 2H_2O(s) + 2CaCO_3(s) \rightarrow Ca_8H_2(PO_4)_6 - 5H_2O(s) + 2CO_2(g) + 9H_2O(aq) \quad (7)$$

$$Ca_8H_2(PO_4)_6 - 5H_2O(s) + 2CaCO_3(s) \rightarrow Ca_{10}(PO_4)_6(OH)_2(s) + 2CO_2(g) + 5H_2O(aq) \quad (8)$$

Melilite

Melilite is a typical amorphous product analogous in composition to the silicoaluminates present in fly ash. The chemical formula of the melilite we studied was $Ca_2AlSi_2O_7$, with some substitution of cations for Na, Fe and Mg. Phosphoric acid reacted partially with melilite, as illustrated in Figure 11. The extent of reaction depended on the acid concentration. With 907 mmol l^{-1} phosphoric acid, 245 mmol l^{-1} phosphate was consumed, leaving three-quarters of the phosphate in solution after an 80 min period. Initially, our melilite suspension had a pH value of 10.2. This value fell to 2.8 immediately following addition of phosphoric acid, and then levelled to a plateau of pH 3.8 after 3 min of mixing. The temperature rises were 5.9°C and 10.8°C for 453 mmol l^{-1} and 907 mmol l^{-1} phosphoric acid, respectively. This is significantly more than the 1.5°C and 3°C rises due to acid dilution and implies an exothermal reaction for melilite and phosphoric acid.

The changes in soluble calcium, aluminium and silicon are reported as a function of time and initial phosphate concentrations in Figure 12. Without phosphoric acid, calcium dissolved up to 0.8 mmol l^{-1} (detection limit 0.05 mmol l^{-1}), and both silicon and aluminium stayed below the detection limits (0.1 and 0.01 mmol l^{-1}, respectively). However, with phosphoric acid, the concentration of aluminium increased to 105 mmol l^{-1} and then decreased

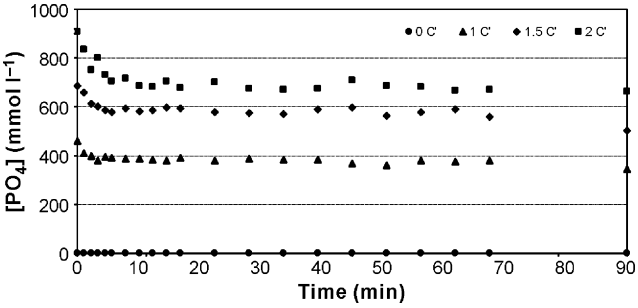

Figure 11. PO_4^{3-} in solution during reaction between H_3PO_4 and melilite at 20°C and 400 rpm. C′: 453 mmol l^{-1} of phosphoric acid.

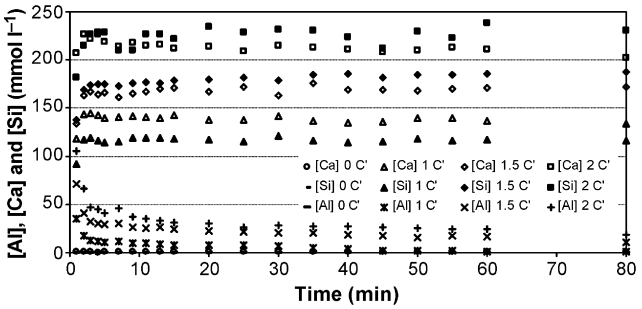

Figure 12. Al^{3+}, Ca^{2+} and Si^{4-} in solution during reaction between H_3PO_4 and melilite at 20°C and 400 rpm. C′: 453 mmol l^{-1} of phosphoric acid.

rapidly during the following 5 min to a low value near 18 mmol l^{-1} for 907 mmol l^{-1} phosphoric acid. Calcium and silicon concentrations both rose to similar values depending on acid concentration. For 907 mmol l^{-1} acid added, concentrations were above 200 mmol l^{-1}. These relatively high calcium concentrations were due to the acidic pH. For silicon, the concentrations were two orders of magnitude higher than those observed with pure silica. It may be concluded phosphoric acid mainly reacts with melilite by acid dissolution followed by aluminium phosphate precipitation.

XRD analysis of melilite showed an almost completely amorphous structure with one weak peak at 2θ values of 32°. After the phosphoric acid reaction, this peak disappeared, but an amorphous halo remained. Once again, aluminium phosphate precipitated as an amorphous solid. Considering that melilite did dissolve to liberate silica, aluminium and calcium and looking at the amount of phosphate consumed, we conclude the amorphous precipitate contains two times more phosphate than aluminium.

Comparison Between the Different Model Components

Some components of fly ash, such as silica and calcium sulphate particles are inert towards phosphoric acid solutions. Aluminium containing compounds react with phosphoric acid to form very insoluble amorphous species. Such precipitates practically inhibit further reaction with excess acid. However, some dissolution occurs followed by precipitation. Overall, some 15–25% of the phosphoric acid introduced reacted or formed surface adsorbed species containing aluminium. This must be taken into account when predicting the amount of phosphoric acid needed to react with calcium ions or heavy metal ions to be immobilized. Calcium carbonate and hydroxide are the most reactive species towards phosphoric acid. All the acid introduced could be used to form various calcium phosphate salts. At neutral pH values, apatites are predicted to be the favoured end species (Meyer and Weatherall, 1982).

The model compounds singled out in this study illustrate how phosphoric acid reacts differently with each one of them. The binary reactions observed were designed to reflect the respective concentrations found in typical fly ashes. However, in the real case of fly ashes, the viscosity of the reaction mixture is higher and adsorption on the more inert components will slow the reaction with the more reactive particles. Therefore, the distribution of competing reactions combined with the diffusion of phosphoric acid conjugate to slow down and smooth out the consumption of soluble phosphate and the formation of amorphous gel precipitates. The introduction of phosphoric acid into fly ash first neutralizes available bases then dissociates fragile components. But in the end, fly ashes overwhelm the phosphoric acid and completely neutralize all available acidities. The dissolution and precipitation sequence of events perfectly explains the experimental pH profiles observed. Other authors have reported that acidification of apatite suspensions helps to promote the formation of insoluble lead phosphates (Zhang and Ryan, 1999). The advantage of using phosphoric acid as a stabilizing agent lies in the simplicity of use, broad spectrum reactivity and self control of final pH.

Even though the reactions proceed quickly with the pure calcium compounds studied, the rates could be slowed by the dissolution step and by interactions between elements. For instance, transient species including soluble calcium hydrogenophosphates may be formed as well as soluble calcium silicophosphates, depending on pH and availability of dissolved ions.

CONCLUSION

The chemical treatment of fly ashes with phosphoric acid proceeds in several steps: initially fast neutralization of basic hydroxides occurs. Then, excess phosphoric acid is consumed rapidly to precipitate insoluble salts. Finally the remaining phosphate binds to metal oxides which transform progressively into stable species. The reaction between calcium carbonate and phosphoric acid seems to best illustrate the sequence of events with corresponding phosphoric acid consumption kinetics, pH evolution and temperature rise. The formation of amorphous calcium phosphate by this reaction, which tends to transform into hydroxyapatite, shows that this treatment may effectively trap heavy metals in a stable mineralogical phase.

The complex rheological behaviour observed for phosphoric acid treated fly ash may also be attributed to the formation of amorphous gel type networks (Bournonville and Nzihou, 2002; Bournonville *et al.*, 2003). Trace heavy metal ions may react directly with phosphoric acid or may be trapped at any stage inside the apatite matrix being formed during the chemical treatment (Chen *et al.*, 1997; Da Rocha *et al.*, 2002). Formation of mixed phosphates or heavy metal substituted apatites will effectively consume phosphoric acid and immobilise the trace elements. Phosphate treatment of fly ash has been previously reported as an effective method of stabilisation (Derie and Depaus, 1999; Lyons, 2000). Our kinetic results show that the actual behaviour of the fly ashes with respect to phosphoric acid reflects the sum of many different reactions, as illustrated by the reaction of simple compounds which yield several end products. In any case, practically all the soluble phosphate is consumed within the first 30 min of mixing. Less than 1 h is needed to stabilize the pH and the evolution of other soluble species. However, slower conversion of the phosphate products will continue to produce still more stable mineral species. This is one advantage of the phosphate stabilization process which confirms its unique and broad interest in the treatment of heavy metal polluted wastes such as fly ashes.

REFERENCES

Admassu, W. and Breese, T., 1999, Feasibility of using natural fishbone apatite as a substitute for hydroxyapatite in remediating aqueous heavy metals, *Journal of Hazardous Materials*, B69: 187–196.

Andac, M. and Glasser, F.P., 1998, The effect of test conditions on the leaching of stabilised MSWI-fly ash in Portland cement, *Waste Management*, 18: 309–319.

Barth, E.F. and Barich, J.J., 1995, Evaluation techniques solidification-stabilization processes, *Proceeding of congrès international sur les Procédés de Solidification et de Stabilisation des déchets*, Nancy, France, 391–394.

Bernard, L., Freche, M., Lacout, J.L. and Biscans, B., 1999, Preparation of hydroyapatite by neutralization at low temperature—influence of purity of the raw material, *Powder Technol*, 103: 19–25.

Bernard, L., Freche, M., Lacout, J.L. and Biscans, B., 2000, Modeling of the dissolution of calcium hydroxyde in the preparation of hydroxyapatite by neutralisation, *Chem Eng Sci*, 55: 5683–5692.

Bournonville, B., Nzihou, A. and Sharrock, P., 2001, Rheological behaviour and calorimetry of fly ash suspension during phosphate reaction, *Proceeding 6th World Congress of Chemical Engineering*, Melbourne, Australia.

Bournonville, B., 2002, Stabilisation des métaux lourds dans les cendres volantes d'incinération—comportement rhéologique, cinétique de phosphatation et évaluation du procédé, Thesis, Université de Perpignan, France.

Bournonville, B. and Nzihou, A., 2002, Rheology of non-Newtonian suspensions of fly ash: effect of concentration, yield stress and hydrodynamic interactions, *Powder Technol*, 128(2–3): 148–158.

Bournonville, B., Bailliez, S., Nzihou, A. and Sharrock, P. 2003, A beneficial reuse of incinerator fly ash following phosphate treatment: reaction kinetics and control of properties by calcination, *Proceeding Beneficial Use of Recycled Materials in Transportation Applications*, Air & Waste Management Association, Arlington, Virginia, USA, 791–800.

Bournonville, B., Nzihou, A., Sharrock, P. and Depelsenaire, G., 2004, Stabilisation of heavy metal containing dusts by reaction with phosphoric acid: study of the reactivity of fly ash, *Journal of Hazardous Materials*, B116: 65–74.

Chen, X., Wright, J.V., Conca, J.L. and Peurrung, L.M., 1997, Effect of pH on heavy metal sorption on mineral apatite, *Environ Sci Technol*, 31(3): 624–631.

Crannell, B.S., Eighmy, T.T., Krzanowski, J.E., Eusden Jr, J.D., Shaw, E.L. and Francis, C.A., 2000, Heavy metal stabilization in municipal solid waste combustion bottom ash using soluble phosphate, *Waste Management*, 20: 135–148.

Da Rocha, N.C.C., De Campos, R.C., Rossi, A.M., Moreira, A.L., Barbosa, A.D.F. and Moure, G.T., 2002, Cadmium uptake by hydroxyapatite synthesized in different conditions and submitted to thermal treament, *Environ Sci Technol*, 36: 1630–1635.

Derie, R., 1996, A new way to stabilize fly ash from municipal incinerators, *Waste Management*, 16(8): 711–716.

Derie, R. and Depaus, C., 1999, Sur le comportement des polluants minéraux et organiques au cours du procédé NEUTREC d'inertage des cendres volantes d'incinérateurs d'ordures ménagères, *Proceeding of Stab & Env 99*, Montpellier, France, 269–273.

Eighmy, T.T., Crannell, B.S., Butler, L.G., Cartledge, F.K., Emery, E.F., Oblas, D., Krzanowski, J.E., Eusden Jr, J.D., Shaw, E.L. and Francis, C.A., 1997, Heavy metal stabilization in municipal solid waste combustion dry scrubber residue using soluble phosphate, *Environ Sci Technol*, 31(11): 3330–3338.

Fuller, C.C., Bargar, J.R., Davis, J.A. and Piana, M.J., 2002, Mechanisms of uranium interactions with hydroxyapatite: implications for groundwater remediation, *Environ Sci Technol*, 36: 158–165.

Gilbert, R.L. and Moreno, E.C., 1965, Dissolution of phosphate rock by mixtures of sulfuric and phosphoric acids, *Ind Eng Chem, Process Des Dev*, 4(4): 368–371.

Gioia, F., Mura, G. and Vioia, A., 1977, Analysis, simulation, and optimization of the hemihydrate process for the production of phosphoric acid from calcareous phosphorites, *Ind Eng Chem, Process Des Dev*, 16(3): 390–399.

Haguenauer, B., Nion, S., Schreiner, D., Albouy, M., Delétie, P., Damien, A. and Gutierrez, G., 1995, L'apatite des dents de requin fossiles de 60 millions d'années, garante du piégeage des métaux toxiques ou radioactifs, *Proceeding of Congres International sur les Procédés de Solidification et de Stabilisation des déchets*, Nancy, France, 506–509.

Hudson, R.B. and Dolan, M.J., 1982, Phosphoric acids and phosphates, *Encyclopedia of Chemical Technology*, Wiley-Interscience, 17: 426–472.

Iretskaya, S., Nzihou, A., Zahraoui, C. and Sharrock, P., 1999, Metal leaching from MSW fly ash before and after chemical and thermal treatments, *Environ Prog*, 18(2): 144–148.

Laperche, V., Traina, S.J., Gaddam, P. and Logan, T.J., 1996, Chemical and mineralogical characterizations of Pb in a contaminated soil: reactions with synthetic apatite, *Environ Sci Technol*, 30: 3321–3326.

Le Forestier, L. and Libourel, G., 1998, Characterization of flue gas residues from municipal solid waste combustors, *Environ Sci Technol*, 32(15): 2250–2256.

Leyva, A.G., Marrero, J., Smichowski, P. and Cicerone, D., 2001, Sorption of antimony onto hydroxyapatite, *Environ Sci Technol*, 35: 3669–3675.

Lyons, M.R., 2000, The use of soluble phosphates to stabilize heavy metals in ash, *Sustainable construction use of incinerator ash*, Proceedings of the International Symposium organized by the Concrete Technology Unit, University of Dundee, UK, 87–96.

Ma, Q.Y., Logan, T.J., Traina, S.J. and Ryan, J.A., 1994a, Effects of NO_3^-, Cl^-, F^-, SO_4^{2-} and CO_3^{2-} on Pb^{2+} immobilization by hydroxyapatite, *Environ Sci Technol*, 28: 408–418.

Ma, Q.Y., Traina, S.J., Logan, T.J. and Ryan, J.A., 1994b, Effects of aqueous Al, Cd, Cu, Fe(II), Ni, and Zn on Pb immobilization by hydroxyapatite, *Environ Sci Technol*, 28: 1219–1228.

Mavropoulos, E., Rossi, A.M., Costa, A.M., Perez, C.A.C., Moreira, J.C. and Saldanha, M., 2002, Studies on the mechanisms of lead immobilization by hydroxyapatite, *Environ Sci Technol*, 36: 1625–1629.

Meyer, J.L. and Weatherall, C.C., 1982, Amorphous to crystalline calcium phosphate phase transformation at elevated pH, *Journal of Colloid and Interface Science*, 89(1): 257–267.

Piantone, P., Bodénan, F., Derie, R. and Depelsenaire, G., 2003, Monitoring the stabilization of municipal solid waste incineration fly ash by phosphatation: mineralogical and balance approach, *Waste Management*, 23(3): 225–243.

Van Kemenade, M.J.J.M. and de Bruyn, P.L., 1987, A kinetic study of precipitation from supersaturated calcium phosphate solutions, *Journal of Colloid and Interface Science*, 118(2): 564–585.

Zhang, P., Ryan, J.A. and Bryndzia, L.T., 1997, Pyromorphite formation from goethite adsorbed lead, *Environ Sci Technol*, 31: 2673–2678.

Zhang, P. and Ryan, J.A., 1998, Formation of pyromorphite in anglesite-hydroxyapatite suspensions under varying pH conditions, *Environ Sci Technol*, 32: 3318–3324.

Zhang, P. and Ryan, J.A., 1999, Transformation of Pb(II) from cerrusite to chloropyromorphyte in the presence of hydroxyapatite under varying conditions of pH, *Environ Sci Technol*, 33: 625–630.

ACKNOWLEDGEMENT

This work was supported by SOLVAY Group (Health Safety Environment Department). This support is gratefully acknowledged.